

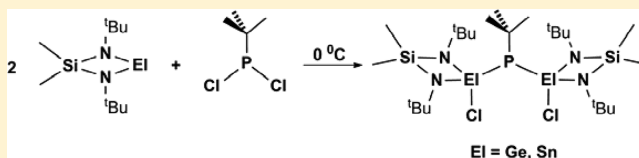
Insertions of Cyclic and Acyclic Germanium and Tin Heterocarbenoids into Phosphorus–Chlorine Bonds: Syntheses, Structures, and Reactivities

Joseph K. West and Lothar Stahl*

Department of Chemistry, University of North Dakota, Grand Forks, North Dakota 58202-9024 United States

Supporting Information

ABSTRACT: Chloro(organo)phosphines are important precursors to diphosphenes and cyclic oligophosphines. Although chloro(organo)phosphines are commonly reduced with bulk metals (e.g., Na, Mg, and Zn), these reactions are much more selective when done homogeneously. To test whether group 14 heterocarbenoid reductions yield isolable insertion products, the mono- and dichloro(organo)phosphines PhPCl_2 (A), Ph_2PCl (B), ${}^t\text{BuPCl}_2$ (C), ${}^t\text{Bu}_2\text{PCl}$ (D), and bis(dichlorophosphino)methane $(\text{PCl}_2)_2\text{CH}_2$ (E) were treated with the cyclic $\text{Me}_2\text{Si}(\mu\text{-N}^t\text{Bu})_2\text{El}$ (El = Ge (1), Sn (2)) and the acyclic $[(\text{Me}_3\text{Si})_2\text{N}]_2\text{El}$ (El = Ge (3), Sn (4)) heterocarbenoids. The sterically least-encumbered phosphines were more reactive, while the cyclic stannylene **2** was the most reactive and the acyclic germylene **3** was the least reactive. All but one of the products were either mono- or diinsertion compounds, the lone exception being a distannane derived from **2**. Semikinetic and structural data suggest that the tetravalent group 14 compounds are formed via an insertion mechanism whose rate depends on the steric bulk of the reaction partners and the nature of the group 14 elements.



1. INTRODUCTION

Phosphorus is sometimes referred to as the “carbon copy” on account of the somewhat similar chemical properties that exist between these two elements.¹ This diagonal relationship, however, is less well developed than that between members of the earlier groups of the periodic table: cf. lithium/magnesium or beryllium/aluminum. Unlike carbon, phosphorus(III) has a lone pair of electrons that renders it Lewis basic and makes it susceptible to redox reactions. The group 15 element does, however, have an undeniable tendency to form phosphorus–phosphorus single and double bonds that mirror certain aspects of organic chemistry. Phosphorus–phosphorus bonds,² just like carbon–carbon bonds, can be generated by the reduction of the corresponding halides. A variety of reducing agents—mainly alkali metals, magnesium, and zinc—have been used for this purpose, although the nature of the metal does seem to matter in the outcomes of the reductions.^{3–7} In contrast to alkyl halide reductions, where species such as R–Mg–X and R–Zn–X are formed,⁸ no such intermediates are obtained for bulk metal reductions of the more reactive halophosphines. The isolation of oxidative addition products in chlorophosphine reduction requires both milder reducing agents and milder conditions.

As long ago as 1983 Bertrand and Veith showed that the cyclic stannylene $\text{Me}_2\text{Si}(\mu\text{-}{}^t\text{BuN})_2\text{Sn}$ reduces dichlorophosphines under extremely mild conditions, $\text{Me}_2\text{Si}(\mu\text{-}{}^t\text{BuN})_2\text{SnCl}_2$ being the only oxidation product.⁹ The subsequent isolation of $[\text{Me}_2\text{Si}(\mu\text{-}{}^t\text{BuN})_2\text{Ge}(\text{Cl})]_3\text{P}$,¹⁰ upon treatment of PCl_3 with $\text{Me}_2\text{Si}(\mu\text{-}{}^t\text{BuN})_2\text{Ge}$, provided clear evidence that such reductions proceed with the intermediacy of insertion products. This conclusion was supported by the work of du

Mont et al., who proved that even GeCl_2 can insert into the P–Cl bonds of chloro(organo)phosphines.^{11–13}

Despite these well-documented cases of group 14 heterocarbenoid insertions into P–Cl bonds, there have been no systematic investigations into these reactions. This dearth of interest is surprising, because although phosphorus–halogen bond transformations lack the general utility of carbon–halogen bond transformations, there are numerous applications for such reactions. For example, the making of phosphorus–phosphorus bonds by milder and hence more selective routes is important in the syntheses of diphosphenes and oligophosphines. Detailed studies of heterocarbenoid insertions into P–Cl bonds may also provide insight into the selective generation of the long-sought phosphinidenes,^{14–16} which are, incidentally, valence isoelectronic with germylenes and stannylenes.

Prior to our investigations no stannylene insertion product into a phosphorus–halogen bond had ever been isolated; they had merely been identified by NMR spectroscopy. A few of the more stable germylene insertion products had been characterized by in situ ${}^1\text{H}$ and ${}^{31}\text{P}$ NMR techniques,¹⁷ but only two of these (vide supra) had been structurally characterized by X-ray techniques.^{10,12} Herein we report on insertions of cyclic and acyclic germanium and tin heterocarbenoids into the phosphorus–chlorine bonds of chloro(organo)phosphines. The emphasis in these studies was on the structures of the products, as well as the relative reactivities of the heterocarbenoids and the phosphine substrates. It will be seen that P–Cl reductions with homologous heterocarbenoids did not

Received: January 8, 2012

Published: February 22, 2012

always give homologous products and that the reaction rates differed significantly, with half-lives ranging from seconds to months. In most cases the metastable insertion products were isolated and fully characterized, thereby more than quadrupling the number of such species.

2. EXPERIMENTAL SECTION

2.1. General Procedures. All manipulations and reactions were carried out under an inert atmosphere of argon, using standard Schlenk techniques. Solvents were dried over and distilled from Na/benzophenone (toluene) and K/benzophenone (THF and hexanes). PhPCl_2 and Ph_2PCl were purchased from Aldrich Chemical Co. and distilled before use. The aliphatic phosphine ${}^t\text{Bu}_2\text{PCl}$ was synthesized using a published procedure, and ${}^t\text{BuPCl}_2$ was prepared similarly, using only 1 equiv of ${}^t\text{BuLi}$.¹⁸ The heterocarbenoids $\text{Me}_2\text{Si}(\mu\text{-N}^t\text{Bu})_2\text{El}$, El = Ge (1), Sn (2),^{19–21} and $[(\text{Me}_3\text{Si})_2\text{N}]_2\text{El}$, El = Ge (3), Sn (4),²² were synthesized according to literature procedures. All ${}^1\text{H}$, ${}^{13}\text{C}$, and ${}^{31}\text{P}$ NMR spectra were recorded on a Bruker Avance 500 NMR spectrometer. The NMR spectra were recorded in C_6D_6 , THF- d_6 , and CD_2Cl_2 , and the chemical shifts, δ , are relative to the solvent peak(s) (e.g., C_6D_6) for ${}^1\text{H}$ and ${}^{13}\text{C}$ spectra and the external standard $\text{P}(\text{OEt})_3$ for ${}^{31}\text{P}$ spectra. Midwest Micro Labs, LLC, Indianapolis, IN, and Columbia Analytical Services, Tucson, AZ, performed the elemental analyses.

2.2. Syntheses. $[\text{Me}_2\text{Si}(\mu\text{-}^t\text{BuN})_2\text{GeCl}]_2\text{PPh}$ (5). In a 50 mL flask, PhPCl_2 (0.27 mL, 2.0 mmol) was stirred in pentane (4 mL) at 0 °C. A 2.0 M toluene solution of $\text{Me}_2\text{Si}(\mu\text{-}^t\text{BuN})_2\text{Ge}$ (2.0 mL, 4.0 mmol) was added by syringe over 15 min. After 2 h the reaction mixture was removed from the cold bath and stirred at room temperature overnight. Colorless crystals were obtained in an almost quantitative yield from a pentane/toluene solution at 3 °C. Yield: 1.39 g (96%). Mp: 112–114 °C. Anal. Calcd for $\text{C}_{26}\text{H}_{53}\text{Cl}_2\text{Ge}_2\text{N}_4\text{PSi}_2$ (725.06): C, 43.07; H, 7.37; N, 7.73. Found: C, 43.10; H, 7.30; N, 7.67. ${}^1\text{H}$ NMR (500 MHz, CD_2Cl_2 , 25 °C): δ 0.35 (s, 6 H, SiMe), 0.44 (s, 6 H, SiMe), 1.19 (s, 36 H, N^tBu), 7.34 (m, 1 H, $p\text{-C}_6\text{H}_5$), 7.36 (m, 2 H, $m\text{-C}_6\text{H}_5$), 7.94 (m, 2 H, $o\text{-C}_6\text{H}_5$). ${}^{13}\text{C}\{^1\text{H}\}$ NMR (125.8 MHz, CD_2Cl_2 , 25 °C): δ 5.43 (s, SiMe), 6.87 (s, SiMe), 34.5 (s, NCMe_3), 52.8 (s, NCMe_3), 128.6 (d, ${}^1J_{\text{PC}} = 13.8$ Hz, PC), 128.9 (d, ${}^3J_{\text{PC}} = 8.8$ Hz, $m\text{-C}_6\text{H}_5$), 129.9 (s, $p\text{-C}_6\text{H}_5$), 137.2 (d, ${}^2J_{\text{PC}} = 17.6$ Hz, $o\text{-C}_6\text{H}_5$). ${}^{31}\text{P}\{^1\text{H}\}$ NMR (202.5 MHz, CD_2Cl_2 , 25 °C): δ -55.2.

$[(\text{Me}_3\text{Si})_2\text{N}]_2\text{Sn}(\text{Cl})\text{P}(\text{Ph})_2$ (6). In a 100 mL flask, $[(\text{Me}_3\text{Si})_2\text{N}]_2\text{Sn}$ (2.79 g, 6.24 mmol) was stirred in 10 mL of hexanes at 0 °C. Exactly 1.56 mL of a 2.0 M toluene solution of PhPCl_2 (3.12 mmol) was added by syringe over 20 min, producing a yellow solution with a significant amount of a yellow precipitate. Bright yellow crystals were obtained in several fractions from a concentrated THF solution at 3 °C. Yield: 2.62 g (72%). Mp: 220–221 °C. Anal. Calcd for $\text{C}_{36}\text{H}_{82}\text{Cl}_2\text{N}_4\text{P}_2\text{Si}_8\text{Sn}_2$ (1166.02): C, 37.08; H, 7.09; N, 4.80. Found: C, 37.05; H, 6.81; N, 4.97. ${}^1\text{H}$ NMR (500 MHz, C_6D_6 , 25 °C): δ 0.106 (s, 72 H, SiMe), 7.47 (m, 2 H, $m\text{-C}_6\text{H}_5$), 7.52 (m, 2 H, ${}^3J_{\text{PH}} = 1.9$ Hz, $o\text{-C}_6\text{H}_5$), 7.98 (m, 1 H, $p\text{-C}_6\text{H}_5$). ${}^{13}\text{C}\{^1\text{H}\}$ NMR (125.8 MHz, C_6D_6 , 25 °C): δ 1.54 (s, SiMe), 130.31 (s, $m\text{-C}_6\text{H}_5$), 130.72 (s, $o\text{-C}_6\text{H}_5$), 131.76 (s, $p\text{-C}_6\text{H}_5$). ${}^{31}\text{P}\{^1\text{H}\}$ NMR (202.5 MHz, C_6D_6 , 25 °C): δ -28.5 (${}^1J_{\text{P}^{191}\text{Sn}} = 1470, 1404$ Hz).

$[(\text{Me}_3\text{Si})_2\text{N}]_2\text{Ge}(\text{Cl})\text{PPh}_2$ (8). In a 25 mL two-neck flask, a 2.0 M toluene solution of $[(\text{Me}_3\text{Si})_2\text{N}]_2\text{Ge}$ (1.0 mL, 2.0 mmol) was stirred at 0 °C. A 2.67 M toluene solution of Ph_2PCl (0.75 mL, 2.0 mmol) was added dropwise by syringe over 30 min. The product was isolated as colorless crystals from toluene at 3 °C in a nearly quantitative yield. Yield: 1.15 g (94%). Mp: 126–128 °C. Anal. Calcd for $\text{C}_{24}\text{H}_{46}\text{ClGeN}_2\text{PSi}_4$ (614.04): C, 46.94; H, 7.55; N, 4.56. Found: C, 46.54; H, 7.29; N, 4.34. ${}^1\text{H}$ NMR (500 MHz, C_6D_6 , 25 °C): δ 0.30 (s, 36 H, SiMe₃), 7.01–7.08 (m, 6 H, $o, m\text{-C}_6\text{H}_5$), 7.75–7.78 (m, 4 H, $p\text{-C}_6\text{H}_5$). ${}^{13}\text{C}\{^1\text{H}\}$ NMR (125.8 MHz, C_6D_6 , 25 °C): δ 7.18 (s, SiMe₃), 129.34 (d, ${}^2J_{\text{PC}} = 84.3$ Hz, $o\text{-C}_6\text{H}_5$), 134.88 (d, ${}^3J_{\text{PC}} = 22.6$ Hz, $m\text{-C}_6\text{H}_5$), 136.91 (d, ${}^4J_{\text{PC}} = 21.4$ Hz, $p\text{-C}_6\text{H}_5$). ${}^{31}\text{P}\{^1\text{H}\}$ NMR (202.5 MHz, C_6D_6 , 25 °C): δ -16.0.

$[\text{Me}_2\text{Si}(\mu\text{-}^t\text{BuN})_2\text{SnCl}]_2\text{P}^t\text{Bu}$ (9). In a 50 mL two-neck flask, ${}^t\text{BuPCl}_2$ (0.467 g, 2.94 mmol) was stirred in 10 mL of hexanes at 0 °C.

$\text{Me}_2\text{Si}(\mu\text{-}^t\text{BuN})_2\text{Sn}$ (1.875 g, 5.87 mmol) was added dropwise by syringe over 1.5 min. The solution became yellow-orange during the addition. The flask was removed from the cold bath after 40 min of stirring at 0 °C. X-ray-quality, yellow crystals were obtained in multiple fractions from the reaction solution at 3 °C after several days. Yield: 1.351 g (58%). Mp: 112–116 °C. Anal. Calcd for $\text{C}_{24}\text{H}_{57}\text{Cl}_2\text{N}_4\text{PSi}_2\text{Sn}_2$ (797.21): C, 36.16; H, 7.21; N, 7.03. Found: C, 36.10; H, 7.22; N, 6.78. ${}^1\text{H}$ NMR (500 MHz, C_6D_6 , 25 °C): δ 0.41 (s, 6 H, SiMe), 0.48 (s, 6 H, SiMe), 1.36 (s, 36 H, N^tBu), 1.61 (d, 9 H, ${}^3J_{\text{PH}} = 15$ Hz, ${}^4J_{\text{SnH}} = 10$ Hz, P^tBu). ${}^{13}\text{C}\{^1\text{H}\}$ NMR (125.8 MHz, C_6D_6 , 25 °C): δ 6.88 (s, ${}^3J_{\text{SnC}} = 50$ Hz, SiMe), 7.94 (s, ${}^3J_{\text{SnC}} = 50$ Hz, SiMe), 35.9 (d, ${}^3J_{\text{SnC}} = 41.5$ Hz, ${}^2J_{\text{PC}} = 12.6$ Hz, PCMe_3), 36.5 (s, ${}^3J_{\text{SnC}} = 34.0$ Hz, NCMe_3), 38.9 (d, ${}^1J_{\text{PC}} = 37.7$ Hz, ${}^2J_{\text{SnC}} = 31.5$ Hz, PCMe_3), 53.6 (s, ${}^2J_{\text{SnC}} = 20.6$ Hz, NCMe_3). ${}^{31}\text{P}\{^1\text{H}\}$ NMR (202.5 MHz, C_6D_6 , 25 °C): δ 7.1 (${}^1J_{\text{P}^{191}\text{Sn}} = 1616, 1543$ Hz).

$[\text{Me}_2\text{Si}(\mu\text{-}^t\text{BuN})_2\text{GeCl}]_2\text{P}^t\text{Bu}$ (10). In a 25 mL two-neck flask, a 1.0 M toluene solution of ${}^t\text{BuPCl}_2$ (2.0 mL, 2.0 mmol) was stirred at 0 °C. A 1.0 M toluene solution of $\text{Me}_2\text{Si}(\mu\text{-}^t\text{BuN})_2\text{Ge}$ (4.0 mL, 4.0 mmol) was added dropwise by syringe over 30 min. The solution was warmed to room temperature and stirred for 3 days. The product was isolated as clear colorless crystals in several fractions from toluene at 3 °C. Yield: 0.813 g (58%). Mp: 117–119 °C. Anal. Calcd for $\text{C}_{24}\text{H}_{57}\text{Cl}_2\text{Ge}_2\text{N}_4\text{PSi}_2$ (705.07): C, 40.88; H, 8.15; N, 7.95. Found: C, 40.52; H, 7.98; N, 7.81. ${}^1\text{H}$ NMR (500 MHz, C_6D_6 , 25 °C): δ 0.407 (br s, 6 H), 0.462 (s, 6 H), 1.415 (s, 36 H), 1.684 (d, 9 H, ${}^3J_{\text{HP}} = 14.9$ Hz). ${}^{13}\text{C}\{^1\text{H}\}$ NMR (125.8 MHz, C_6D_6 , 25 °C): δ 5.83 (s, SiMe), 7.59 (s, SiMe), 34.99 (d, ${}^2J_{\text{PC}} = 12.5$ Hz, P^tBu), 35.06 (s, $\text{NC}(\text{CH}_3)_3$), 38.78 (d, ${}^1J_{\text{PC}} = 32.6$ Hz, PC), 53.41 (s, $\text{NC}(\text{CH}_3)_3$). ${}^{31}\text{P}\{^1\text{H}\}$ NMR (202.5 MHz, C_6D_6 , 25 °C): δ 3.2.

$[(\text{Me}_3\text{Si})_2\text{N}]_2\text{Ge}(\text{Cl})\text{P}^t\text{BuCl}$ (11). In a 50 mL two-neck flask, ${}^t\text{BuPCl}_2$ (0.692 g, 4.35 mmol) was stirred at room temperature in benzene (5 mL). A sample of $[(\text{Me}_3\text{Si})_2\text{N}]_2\text{Ge}$ (1.712 g, 4.35 mmol) was added all at once, and the ensuing solution was stirred for 5 days. The solvent was removed in vacuo, leaving a colorless solid. This was redissolved in a minimal amount of hexanes, affording colorless, X-ray-quality crystals overnight at room temperature. Yield: 1.36 g (56%). Mp: 151–153 °C. Anal. Calcd for $\text{C}_{16}\text{H}_{45}\text{Cl}_2\text{GeN}_2\text{PSi}_4$ (552.40): C, 34.79; H, 8.21; N, 5.07. Found: C, 35.00; H, 8.08; N, 4.96. ${}^1\text{H}$ NMR (500 MHz, C_6D_6 , 25 °C): δ 0.47 (s, 36 H, SiMe₃), 1.36 (d, 9 H, ${}^3J_{\text{PH}} = 14.7$ Hz, P^tBu). ${}^{13}\text{C}\{^1\text{H}\}$ NMR (125.8 MHz, C_6D_6 , 25 °C): δ 7.25 (s, SiMe₃), 28.8 (d, ${}^2J_{\text{PC}} = 17.6$ Hz, $\text{PC}(\text{CH}_3)_3$), 39.9 (d, ${}^1J_{\text{PC}} = 45.3$ Hz, $\text{PC}(\text{CH}_3)_3$). ${}^{31}\text{P}\{^1\text{H}\}$ NMR (202.5 MHz, C_6D_6 , 25 °C): δ 117.5.

$\text{Me}_2\text{Si}(\mu\text{-}^t\text{BuN})_2\text{Sn}(\text{Cl})\text{P}^t\text{Bu}_2$ (12). In a 50 mL two-neck flask, a 1.0 M toluene solution of $\text{Me}_2\text{Si}(\mu\text{-}^t\text{BuN})_2\text{Sn}$ (6.0 mL, 6.0 mmol) was stirred at 0 °C. A 0.67 M toluene solution of ${}^t\text{Bu}_2\text{PCl}$ (4.0 mL, 9.0 mmol) was added dropwise by syringe over 25 min. The solution was heated to 60 °C and stirred for 17 days. The product was isolated as yellow crystals from toluene at 3 °C. Yield: 2.65 g (88%). Mp: 128–129 °C. Anal. Calcd for $\text{C}_{18}\text{H}_{42}\text{ClN}_2\text{PSiSn}$ (499.76): C, 43.26; H, 8.47; N, 5.61. Found: C, 43.05; H, 8.20; N, 5.61. ${}^1\text{H}$ NMR (500 MHz, C_6D_6 , 25 °C): δ 0.350 (s, 3 H, SiMe), 0.544 (s, 3 H, SiMe), 1.375 (s, 18 H, N^tBu), 1.393 (d, 18 H, ${}^3J_{\text{PH}} = 12.4$ Hz, P^tBu). ${}^{13}\text{C}\{^1\text{H}\}$ NMR (125.8 MHz, C_6D_6 , 25 °C): δ 7.23 (s, SiMe), 8.52 (s, SiMe), 33.66 (d, P^tBu_2 , ${}^2J_{\text{PC}} = 13.5$ Hz), 36.5 (s, N^tBu), 36.8 (d, ${}^1J_{\text{PC}} = 37.3$ Hz, PC), 53.27 (s, NC). ${}^{31}\text{P}\{^1\text{H}\}$ NMR (202 MHz, C_6D_6 , 25 °C): δ 92.8 (${}^1J_{\text{P}^{191}\text{Sn}} = 1734, 1657$ Hz).

$\text{Me}_2\text{Si}(\mu\text{-}^t\text{BuN})_2\text{Ge}(\text{Cl})\text{P}^t\text{Bu}_2$ (13). In a 50 mL two-neck flask, a 1.0 M toluene solution of $\text{Me}_2\text{Si}(\mu\text{-}^t\text{BuN})_2\text{Ge}$ (5.0 mL, 5.0 mmol) was treated dropwise at room temperature with a 0.67 M toluene solution of ${}^t\text{Bu}_2\text{PCl}$ (7.46 mL, 5.0 mmol), which was added by syringe over 20 min. The solution was kept stirring at 70 °C for 39 days. The product was isolated as colorless crystals from hexanes at -8 °C. Yield: 0.431 g (19%). Mp: 130–132 °C. Anal. Calcd for $\text{C}_{18}\text{H}_{42}\text{ClGeN}_2\text{PSi}$ (453.69): C, 47.65; H, 9.33; N, 6.17. Found: C, 47.24; H, 9.36; N, 6.02. ${}^1\text{H}$ NMR (500 MHz, C_6D_6 , 25 °C): δ 0.41 (s, 3 H, SiMe), 0.50 (s, 3 H, SiMe), 1.19 (s, 18 H, N^tBu), 1.23 (d, 18 H, ${}^3J_{\text{PH}} = 12.5$ Hz, P^tBu). ${}^{13}\text{C}\{^1\text{H}\}$ NMR (125.8 MHz, C_6D_6 , 25 °C): δ 7.37 (s, SiMe), 8.43 (s, SiMe), 33.27 (d, P^tBu_2 , ${}^2J_{\text{PC}} = 13.6$ Hz), 35.8 (s, N^tBu), 36.3 (d, ${}^1J_{\text{PC}} = 37.3$ Hz, PC), 53.02 (s, NC). ${}^{31}\text{P}\{^1\text{H}\}$ NMR (202 MHz, C_6D_6 , 25 °C): δ 63.51.

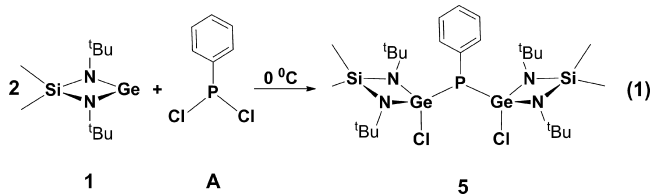
$[(\text{Me}_2\text{Si}(\mu\text{-N}^t\text{Bu})_2\text{Ge}(\text{Cl}))_2\text{P}]_2\text{CH}_2$ (**14**). In a 50 mL three-neck flask, $\text{Me}_2\text{Si}(\mu\text{-}^t\text{BuN})_2\text{Ge}$ (0.557 g, 2.04 mmol) was stirred in hexanes at -78°C . $(\text{Cl}_2\text{P})_2\text{CH}_2$ (0.069 mL, 0.51 mmol) was added via syringe dropwise over 9 min. The reaction solution changed from pale yellow to colorless. After it was warmed to room temperature, a white precipitate appeared. All solvent was removed, and the solid was redissolved in toluene. Clear, colorless, X-ray-quality crystals were obtained from toluene at ca. 3°C after a few days. Yield: 0.350 g (52%). Mp: 188°C dec. Anal. Calcd for $\text{C}_{41}\text{H}_{98}\text{Cl}_4\text{Ge}_4\text{N}_8\text{P}_2\text{Si}_4$ (1309.93): C, 37.59; H, 7.54; N, 8.55. Found: C, 37.80; H, 7.39; N, 8.44. ^1H NMR (500 MHz, C_6D_6 , 25°C): δ 0.455 (s, 12H, SiMe), 0.539 (s, 12H, SiMe), 1.443 (s, 72H, ^tBu), 3.623 (t, 2H, PCH_2P , $^2J_{\text{PH}} = 3.15$ Hz). $^{13}\text{C}\{^1\text{H}\}$ NMR (125.8 MHz, C_6D_6 , 25°C): δ 6.19 (s, SiMe), 7.16 (s, SiMe), 12.13 (t, PCH_2P , $^1J_{\text{PC}} = 157$ Hz), 35.16 (s, NCCH_3), 52.97 (s, NCCH_3). $^{31}\text{P}\{^1\text{H}\}$ NMR (202.5 MHz, C_6D_6 , 25°C): δ -51.9 .

2.3. X-ray Crystallography. Suitable single crystals of **5–14** were coated with Paratone N oil, affixed to Mitegen or Litholoop crystal holders, and centered on the diffractometer under a stream of cold nitrogen. Reflection intensities were collected with a Bruker Apex diffractometer, equipped with an Oxford Cryosystems 700 Series Cryostream cooler, operating at 173 K. Data were measured with ω scans of 0.3° per frame for 20 s until complete hemispheres of data had been collected. Data were retrieved using SMART software and reduced with SAINT-plus,²³ which corrects for Lorentz and polarization effects and crystal decay. Empirical absorption corrections were applied with SADABS.²⁴ The structures were solved by direct methods with SHELXS-97 and refined by full-matrix least-squares methods on F^2 with SHELXL-97.²⁵

3. RESULTS AND DISCUSSION

3.1.1. Syntheses and Structures. Reactions of Chloro(phenyl)phosphines with Group 14 Heterocarbonyls. Previous NMR spectroscopic studies on reductions of halo(organo)phosphines with the cyclic diaminogermynes and -stannylenes **1** and **2**, respectively, had detected the intermediacy of both short-lived and persistent oxidative addition products.¹⁷ Although none of these intermediates had been fully characterized, the studies clearly demonstrated that steric bulk on phosphorus slows the reaction rates and that germylene insertions are slower than those of the corresponding stannylenes. These findings served as benchmarks for our synthetic studies, and we began our investigation by repeating the reduction of dichloro(phenyl)phosphine with the cyclic stannylene **2**.

The reaction of dichloro(phenyl)phosphine (**A**) with 2 equiv of **2** did indeed yield only the cyclic oligophosphines $(\text{PhP})_4$ and $(\text{PhP})_5$ ²⁶ but no characterizable tin-containing product, even when done at -78°C . The germylene analogue **1** reacted significantly more slowly than **2**, as shown in eq 1, the reaction

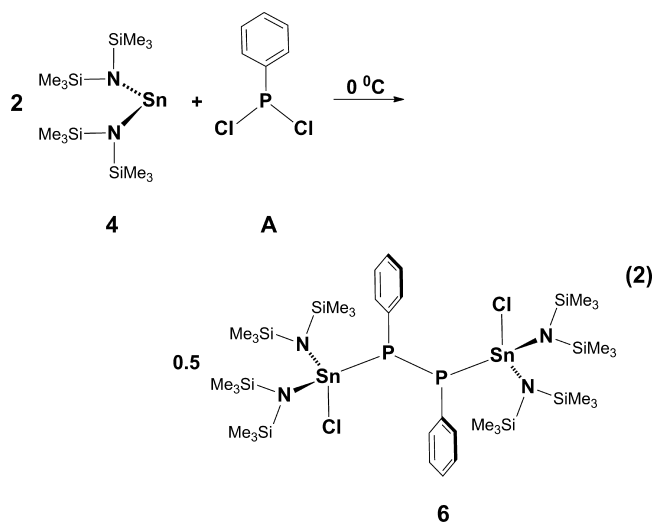


requiring 1 h at 0°C and affording the diinsertion product **5** in almost quantitative yields. Because the intermediate **5** was sufficiently kinetically stable, no cyclic oligophosphines or other phosphorus–phosphorus-bonded species were isolated, nor were they observed by NMR techniques. As is typical for compounds with direct phosphorus–germanium bonds, the thermally stable, colorless **5** exhibited a high-field-shifted signal at -55.2 ppm in the ^{31}P NMR spectrum. Recrystallization of the

bis(chlorogermyl)phenylphosphine **5** from a pentane/toluene mixture gave colorless crystals which were subjected to a single-crystal X-ray analysis. The crystal data and collection and refinement parameters for **5** are given in Table 1, while its solid-state structure is depicted in Figure 1. A normal-length P–C bond (1.837(3) Å) connects the phenyl group to a pyramidal central phosphorus atom that also bears two bulky chlorogermyl moieties, which are attached through two almost equidistant P–Ge bonds of 2.3315(8) and 2.3226(8) Å.

The phosphorus–germanium bonds are only slightly longer than in the tri-insertion product $[\text{Me}_2\text{Si}(\mu\text{-}^t\text{Bu})_2\text{Ge}(\text{Cl})]_3\text{P}^{10}$ and the di-insertion product (adamantyl) $\text{P}(\text{GeCl}_2)_2$,¹² where their average lengths were determined to be 2.310(4) and 2.3100(14) Å, respectively. Despite the steric bulk of the chlorogermyl substituents, the bond angles about phosphorus are close to those expected for an sp^3 -hybridized atom, ranging from $103.85(10)$ to $108.78(3)^\circ$, with an angle sum of 317.87° . This is in contrast to the larger Ge–P–Ge angles in $[\text{Me}_2\text{Si}(\mu\text{-}^t\text{Bu})_2\text{Ge}(\text{Cl})]_3\text{P}$, whose values sum to $345.0(2)^\circ$, consistent with a much flatter pyramid that approaches a trigonal-planar arrangement.¹⁰

The reaction of acyclic germylene **3** with **A** was not as clean as that with **1**, giving instead a complex product mixture. Although a monoinsertion intermediate was identified spectroscopically, the reaction ultimately yielded the cyclic oligophosphines $(\text{PhP})_n$, $n = 4, 5$, as the only identifiable products.



In contrast, and as eq 2 shows, the more reactive acyclic stannylene **4** did furnish an isolable insertion product, albeit not the expected one. It was not possible to assign a structure to this insertion product by NMR spectroscopy alone, but fortunately copious amounts of bright yellow crystals were available, and one of these was subjected to a single-crystal X-ray analysis. Pertinent crystal and refinement data for **6** are collected in Table 1, while selected bond parameters appear in the caption of Figure 2. The thermal ellipsoid plot shows that **6** is not a conventional monoinsertion product, but rather a bulky diphosphine that was likely created in a reaction step that followed an initial insertion.

The compound is a symmetrical diphosphine whose most intriguing features are the two bulky (diamino)(chloro)stannyl substituents. Despite this steric bulk, the phosphorus atoms feature surprisingly small bond angles, which range from $99.3(6)$ to $103.631(17)^\circ$, thereby creating highly pyramidalized phosphorus atoms that are connected by a normal-length P–P

Table 1. Crystallographic Data for 5–14

	5	6	7	8	9	10
chem formula	C ₂₆ H ₄₇ Cl ₂ Ge ₂ N ₄ PSi ₂	C ₃₆ H ₈₂ Cl ₂ N ₄ P ₂ Si ₈ Sn ₂	C ₂₀ H ₄₈ Cl ₂ N ₄ Si ₂ Sn ₂	C ₂₄ H ₄₆ ClGeN ₂ PSi ₄	C ₂₄ H ₅₇ Cl ₂ N ₄ PSi ₂ Sn ₂	C ₂₄ H ₅₇ Cl ₂ Ge ₂ N ₄ PSi ₂
formula wt	718.91	1166.00	709.08	614.00	797.17	704.97
space group	P2 ₁ /n (No. 14)	P $\bar{1}$ (No. 2)	P2 ₁ /c (No. 14)	P $\bar{1}$ (No. 2)	P $\bar{1}$ (No. 2)	P2 ₁ /c (No. 14)
T, °C	−100	−100	−100	−100	−100	−100
a, Å	17.330(3)	9.5087(10)	16.175(10)	9.0100(10)	12.4363(14)	16.782(3)
b, Å	10.0397(16)	10.5988(16)	12.434(7)	11.5526(13)	16.8886(19)	18.699(3)
c, Å	22.406(4)	15.3895(15)	17.246(10)	17.337(2)	19.353(2)	11.7227(19)
α , deg	90	75.362(2)	90	89.039(2)	93.611(2)	90
β , deg	107.715(2)	78.652(2)	108.827(9)	78.051(2)	106.664(2)	100.186(2)
γ , deg	90	70.7470(10)	90	67.828(2)	100.286(2)	90
V, Å ³	3713.5(10)	1405.7(2)	3283(3)	1631.2(3)	3803.3(7)	3620.7(10)
Z	4	1	4	2	4	4
ρ_{calcd} , g cm ^{−3}	1.286	1.377	1.435	1.250	1.392	1.293
λ , Å	0.710 73	0.710 73	0.710 73	0.710 73	0.710 73	0.710 73
μ , mm ^{−1}	1.891	1.239	1.771	1.232	1.577	1.937
no. of data collected	30 238	11 738	22 017	12 778	29 902	29 782
no. of unique data (R _{int})	8071 (0.0242)	5976 (0.0166)	6175 (0.0346)	6335 (0.0186)	14 842 (0.0167)	7863 (0.0242)
R(F), ^a I > 2 σ (I)	0.0273	0.0248	0.0336	0.0342	0.0316	0.0238
R _w (F ²), ^b all data	0.0834	0.0685	0.1462	0.0922	0.0853	0.0659

	11	12	13	14
chem formula	C ₁₆ H ₄₅ Cl ₂ GeN ₂ PSi ₄	C ₁₈ H ₄₂ ClN ₂ PSiSn ₂	C ₁₈ H ₄₂ ClGeN ₂ PSi	C ₄₁ H ₉₈ Cl ₄ Ge ₄ N ₈ P ₂ Si ₄
formula wt	552.36	499.74	453.64	1309.73
space group	P $\bar{1}$ (No. 2)	P2 ₁ /c (No. 14)	P2 ₁ /c (No. 14)	P $\bar{4}$ (No. 81)
T, °C	−100	−100	−100	−100
a, Å	10.6676(9)	16.0010(14)	11.2153(12)	17.6548(7)
b, Å	11.8453(10)	9.0520(8)	11.8227(13)	17.6548(7)
c, Å	12.1007(11)	18.8509(16)	18.439(2)	10.5683(8)
α , deg	77.3000(10)	90	90	90
β , deg	89.9670(10)	110.2880(10)	93.948(2)	90
γ , deg	76.1580(10)	90	90	90
V, Å ³	1446.1(2)	2561.0(4)	2439.2(5)	3294.1(3)
Z	2	4	4	2
ρ_{calcd} , g cm ^{−3}	1.269	1.296	1.235	1.320
λ , Å	0.710 73	0.710 73	0.710 73	0.710 73
μ , mm ^{−1}	1.471	1.215	1.484	2.124
no. of data collected	12 177	20 788	19 840	45 380
no. of unique data (R _{int})	6172 (0.0130)	5543 (0.0164)	5315 (0.0188)	8131 (0.0212)
R(F), ^a I > 2 σ (I)	0.0226	0.0249	0.0256	0.0218
R _w (F ²), ^b all data	0.0655	0.0676	0.0742	0.0600

$$^a R = \sum |F_o - F_c| / \sum |F_o|, \quad ^b R_w = \{[\sum w(F_o^2 - F_c^2)] / [\sum w(F_o^2)^2]\}^{1/2}; \quad w = 1 / [\sigma^2(F_o)^2 + (xP)^2 + yP], \quad \text{where } P = (F_o^2 + 2F_c^2) / 3.$$

bond (2.2360(10) Å). The elongated phosphorus–tin bonds (2.5706(6) Å) are likely due to the steric bulk of the acyclic chlorostannyl unit. Because the tin–phosphorus bonds are formed by phosphorus hybrid orbitals with high p character, the Sn–P coupling constants are expectedly small, being 1470 and 1404 Hz for the tin-119 and tin-117 isotopes, respectively. Although the tin atoms are approximately tetrahedral, they are surrounded by widely varying bond angles that range from 103.633(17) to 119.35(5)°. The central portion of the molecules is structurally related to the dication of [Ph₃P–PhP–PPh–PPh₃][OTf]₂, reported by Burford et al.,²⁷ and the dianionic tetraphosphorus chains [PhP–PhP–PPh–PPh]^{2−} and [CyP–CyP–PCy–PCy]^{2−}, reported by Grützmacher and co-workers.^{28,29} It therefore comes as no surprise that the bond parameters for the central PhP–PPh moiety in all four compounds are similar, the P–P bonds ranging from 2.163(2) to 2.2360(10) Å, compound **6** having the longest

bond. From eq 2 it is apparent that this dimer cannot be the sole product of the reaction, and this begs the question as to the fate of the second chlorostannyl moiety. A plausible scenario is the loss of a Me₂Si(μ-^tBuN)₂SnCl radical from a diinsertion product, two of which then dimerized to give the dimer compound [Me₂Si(μ-^tBuN)₂(Cl)Sn–Sn(Cl)(μ-^tBu)₂SiMe₂]₂.³⁰

Support for this hypothesis is provided by the isolation of just such a tin dimer, namely **7**, which was obtained in small amounts from the reaction of **B** with 1 equiv of the cyclic stannylene **2**, as shown in eq 3. This reaction is seemingly instantly complete at −78 °C, and just like the reaction of **2** with PhPCl₂, it produces Ph₂PPPPh₂, but here the distannane [Me₂Si(μ-^tBu)₂(Cl)Sn–Sn(Cl)(μ-^tBu)₂SiMe₂]₂ (**7**) was also formed. In previous chlorophosphine reductions by the stannylene **2** only the final oxidation product, namely Me₂Si(μ-^tBu)₂SnCl₂, had been isolated. Although it is not clear

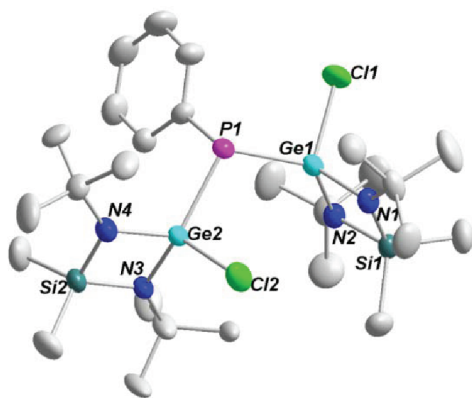


Figure 1. Solid-state structure and partial labeling scheme of **5**. Hydrogen atoms have been omitted, and all non-hydrogen atoms are drawn as 50% probability thermal ellipsoids. Selected bond lengths (Å) and angles (deg): Ge1–P1 = 2.3334(6), Ge2–P1 = 2.3234(6), Ge1–Cl1 = 2.1985(6), Ge2–Cl2 = 2.1924(6), Ge1–N(av) = 1.8276(15), Ge2–N(av) = 1.8314(15); Ge1–P1–Ge2 = 108.792(19), Cl1–Ge1–P1 = 99.40(2), P1–Ge2–Cl2 = 100.29(2), C50–P1–Ge1 = 103.82(6), C50–P1–Ge2 = 105.25(6).

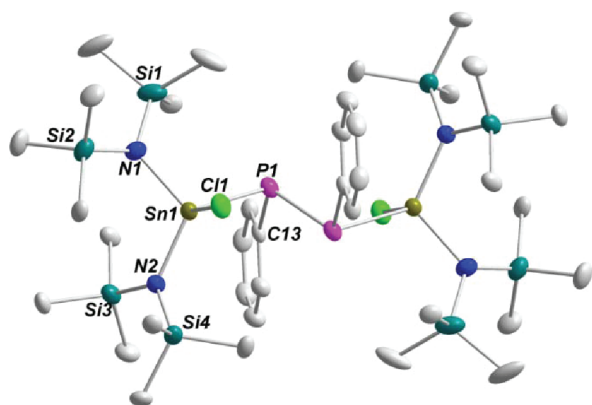


Figure 2. Solid-state structure and partial labeling scheme of centrosymmetric **6**. Hydrogen atoms have been omitted, and all non-hydrogen atoms are drawn as 50% probability thermal ellipsoids. Selected bond lengths (Å) and angles (deg): Sn1–P1 = 2.5706(6), P1–P1' = 2.2360(10), Sn1–Cl1 = 2.3652(5), Sn1–N(av) = 2.0464(16), P1–Cl13 = 1.839(2); Sn1–P1–P1' = 100.57(3), Cl1–Sn1–P1 = 103.631(17), Sn1–P1–Cl13 = 99.34(6), P1'–P1–Cl13 = 100.26(8), N1–Sn1–N2 = 113.87(7), N1–Sn1–Cl1 = 101.87(5), N2–Sn1–Cl1 = 105.79(5), N1–Sn1–P1 = 110.11(5), N2–Sn1–P1 = 119.35(5).

whether all stannylene reductions go through the one-electron process shown in reaction 3, the isolation of **7** lends support to the hypothesis that a similar dimer is produced in reaction 2 above.

The caption of Figure 3 contains selected bond parameters, while crystal and refinement data of **7** are given in Table 1. As the thermal ellipsoid plot of **7** shows, the two chlorostannyl moieties are staggered with respect to each other and connected by a tin–tin bond (2.7799(12) Å) that is slightly shorter than the sum of two covalent tin radii.³¹ Equivalent bond parameters in both units are isometric; this includes the Sn–Cl and Sn–N bonds, which are 2.3631(16) and 2.010(4) Å long on average and thus have lengths similar to those in related compounds.³²

As shown in eq 4, acyclic **3** inserted cleanly into the P–Cl bond of **B** to furnish **8** in almost quantitative yields, while the

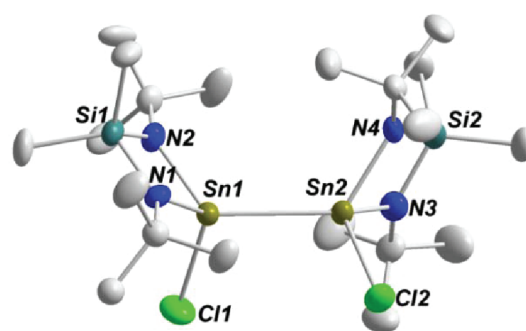
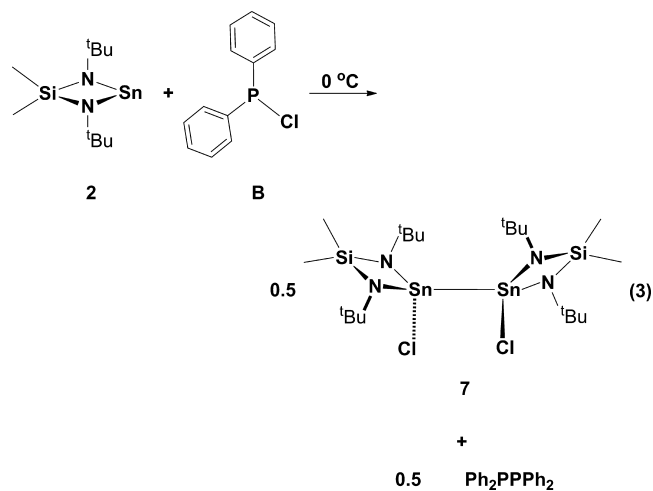
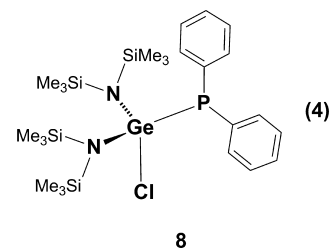
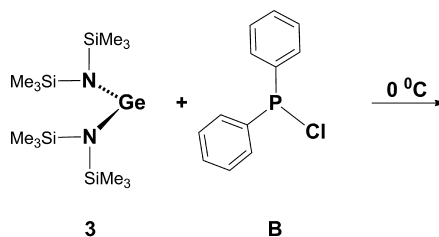


Figure 3. Solid-state structure and partial labeling scheme of **7**. Hydrogen atoms have been omitted, and all non-hydrogen atoms are drawn as 50% probability thermal ellipsoids. Selected bond lengths (Å) and angles (deg): Sn1–Sn2 = 2.7797(12), Sn1–Cl1 = 2.3701(17), Sn2–Cl2 = 2.3561(17), Sn1–N(av) = 2.005(4), Sn2–N(av) = 2.015(4); Cl1–Sn1–Sn2 = 103.94(6), Cl2–Sn2–Sn1 = 106.58(5), N1–Sn1–N2 = 77.1(2), N3–Sn–N4 = 76.7(2).



tin analogue **4** yielded only the diphosphine Ph₂PPP₂ and unidentified metal-containing products. ³¹P NMR spectra showed that the stannylene reaction proceeded with the intermediacy of a tin analogue of **8** that did not persist long enough for isolation. The absence of satellite peaks in germylene derivatives does not allow structural conclusions based on NMR data alone to be made, but the diagnostic shift

of 96.5 ppm to high field was a strong indication that an insertion product had formed.

The solid-state structure of **8**, which is depicted in Figure 4, shows a distorted tetrahedrally coordinated germanium(IV)

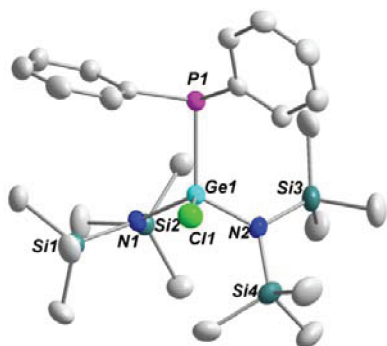


Figure 4. Solid-state structure and partial labeling scheme of **8**. Hydrogen atoms have been omitted, and all non-hydrogen atoms are drawn as 50% probability thermal ellipsoids. Selected bond lengths (Å) and angles (deg): Ge1–P1 = 2.3432(7), Ge1–Cl1 = 2.1918(6), Ge1–N1 = 1.8448(18), Ge1–N2 = 1.8497(18); N1–Ge1–N2 = 112.27(8), N1–Ge1–Cl1 = 110.02(6), N2–Ge1–Cl1 = 103.09(6), N1–Ge1–P1 = 110.84(6), N2–Ge1–P1 = 116.45(6), P1–Ge1–Cl1 = 103.35(2).

center, whose bond angles vary from 103.09(6) to 116.45(6)°. Pertinent crystal and refinement data are collected in Table 1; selected bond parameters appear in the caption of Figure 4. The Ge–Cl and Ge–P bonds are almost identical in length to those in **5**, but the Ge–N bonds in **8** are longer (mean 1.8473(18) Å) due to the much bulkier nitrogen substituents in this acyclic germylene.

3.1.2. Reactions of Chloro(*tert*-butyl)phosphines with Group 14 Heterocarbenoids. Although previously published reports^{9,17} suggested that chloro(alkyl)phosphines undergo carbenoid insertions substantially more slowly than those with aromatic groups, ^tBuPCl₂ reacted rapidly with **2** equiv of **2**, even at 0 °C, as shown in eq 5, to quantitatively afford the

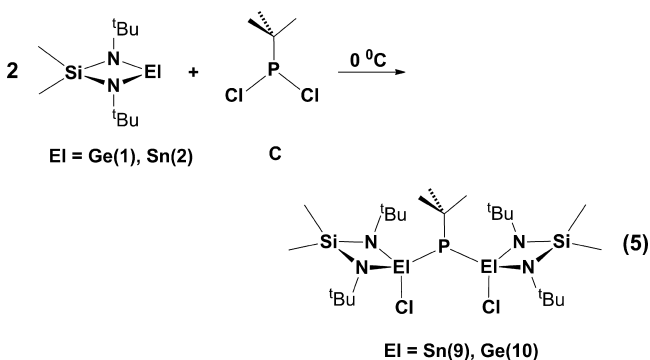


Figure 5. Solid-state structure and partial labeling scheme of one of the two independent molecules of **9**. Hydrogen atoms have been omitted for clarity, and all other atoms are drawn as 50% probability thermal ellipsoids. Selected bond lengths (Å) and angles (deg): Sn1–P1 = 2.5083(8), Sn2–P1 = 2.4937(8), Sn1–Cl1 = 2.3831(10), Sn2–Cl2 = 2.3561(9), Sn1–N(av) = 2.026(3), Sn2–N(av) = 2.026(3) P–C = 1.901(3); Sn1–P1–Sn2 = 104.04(3), Cl1–Sn1–P1 = 99.04(3), P1–Sn2–Cl2 = 103.38(3), Sn1–P1–Cl1 = 109.71(11), Sn2–P1–Cl1 = 106.49(10).

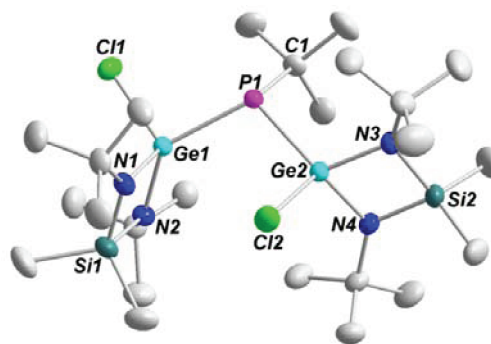


Figure 6. Solid-state structure and partial labeling scheme for **10**. Hydrogen atoms have been omitted, and all other atoms are drawn as 50% probability thermal ellipsoids. Selected bond lengths (Å) and angles (deg): Ge1–P1 = 2.3365(5), Ge2–P1 = 2.3286(5), Ge1–Cl1 = 2.2059(5), Ge2–Cl2 = 2.1836(5), Ge1–N(av) = 1.8373(13), Ge2–N(av) = 1.8357(13); Ge1–P1–Ge2 = 107.664(17), Cl1–Ge1–P1 = 100.494(17), P1–Ge2–Cl2 = 104.535(16), Ge1–P1–Cl1 = 113.33(5), Ge2–P1–Cl1 = 104.50(5).

given in Table 1; selected bond parameters for these compounds appear in their respective figure captions. Compound **9** is the first fully characterized diinsertion product of a stannylene into a dichlorophosphine. The central phosphorus atom is trigonal pyramidally surrounded by its three bulky substituents, as indicated by an angle sum of 320.18°. There are slight asymmetries in both the tin–phosphorus (2.5082(8) and 2.4937(8) Å) and the Sn–Cl bonds (2.3837(9) and 2.3570(9) Å), but the lengths are typical for such bonds.

While the germylene analogue **10** is not isomorphous with **9**, the molecular structures of both products are similar, as Figure 6 shows. The central phosphorus atom in **10** is more crowded and therefore slightly less pyramidal (325.51°) than that in **9**, and this greater steric strain is also reflected in a slightly elongated P–^tBu bond (1.9067(16) Å). Consistent with the difference in the covalent radii of Ge (1.22 Å) and Sn (1.41 Å), both the Ge–P (2.3365(5) and 2.3285(5) Å) and the Ge–Cl bonds (2.2058(5) and 2.1837(5) Å) are 0.18–0.19 Å shorter than those in **10**.

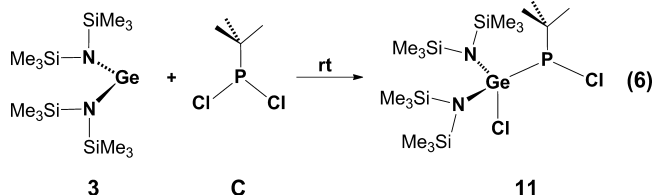
In contrast to cyclic **1** and **2**, the bulkier acyclic heterocarbenoids **3** and **4** did not yield diinsertion products with ^tBuPCl₂. Stannylene **4**, in fact, gave no isolable insertion product at all,

bis(chlorostannyl)-*tert*-butylphosphine **9** after less than 1 h. The integrations of the lone phosphorus signal and those of its tin satellites confirmed the presence of two tin–phosphorus bonds. The cyclic germylene **1** reacted with **C** in a manner analogous to that of **2**, albeit much more slowly, the reaction requiring 3–4 days at room temperature rather than 1 h at 0 °C.

The diinsertion products **9** and **10** are structural analogues, and one of the independent molecules of the tin derivative, **9**, is shown in Figure 5, while Figure 6 depicts the germanium counterpart **10**. Crystal and refinement data for **9** and **10** are

but a monoinsertion intermediate was observed by NMR methods. As is typical for reductions having unstable insertion products, the reaction furnished cyclic tetra- and tri-*tert*-butylcyclophosphines,³³ with a particularly large amount of the latter.

The acyclic germylene **3**, however, did give the stable monoinsertion product **11** in ca. 56% yield, after being allowed to react with **C** for 5 days, as shown in eq 6. Notably, compound



11 is the only product described herein in which an available P–Cl bond did not oxidatively add to a second heterocarbeneid, even though the latter was present in excess.

Compound **11** was isolated in the form of colorless crystals which melt at 151–153 °C; one of these was subjected to an X-ray analysis, the results of which may be seen in Figure 7.

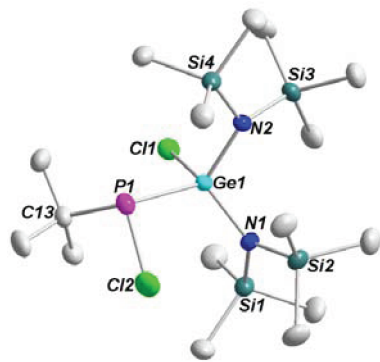


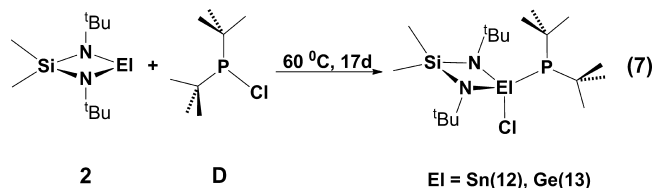
Figure 7. Solid-state structure of and partial labeling scheme for **11**. Hydrogen atoms have been omitted. All atoms are drawn as 50% probability thermal ellipsoids. Selected bond lengths (Å) and angles (deg): Ge1–P1 = 2.3992(4), Ge1–Cl1 = 2.1869(4), Ge1–N1 = 1.8414(11), Ge1–N2 = 1.8468(11), P1–Cl2 = 2.0795(6), P1–Cl3 = 1.8825(15); Ge1–P1–Cl2 = 97.14(2), Cl1–Ge1–P1 = 104.429(15), P1–Ge1–N1 = 114.69(4), P1–Ge1–N2 = 111.49(4), Ge1–P1–Cl3 = 109.82(5), N1–Ge1–N2 = 112.09(5).

Crystal and data collection parameters for **11** are given in Table 1, while selected bond parameters appear in the figure caption.

This monoinsertion product is a close structural relative of **8**, both compounds differing only in the phosphorus substituents, namely phenyl/phenyl in **8** versus *tert*-butyl/chlorine in **11**. The lone Ge–P bond (2.3991(4) Å) in **11** is noticeably longer than that in **8** (2.3432(7) Å), but it is not clear whether this is due to steric or electronic effects. In contrast, the Ge–Cl bonds in **11** and **8** have virtually identical lengths, being 2.1869(4) and 2.1918(6) Å long, respectively.

The di-*tert*-butylchlorophosphine **D** was the by far least reactive chlorophosphine in its oxidative additions to the electron-deficient germanium and tin compounds, requiring elevated temperatures and prolonged reaction periods. Even for the most reactive of the group 14 heterocarbeneids—the cyclic stannylene **2**—the reaction was only 90% complete after 17 days at 60 °C. The acyclic stannylene **4** reacted significantly more slowly, the reaction being only 60% complete after

40 days at 60 °C. Because the cyclic germylene **1** showed no more than 20% conversion, we chose not to investigate the reactivity of this bulky monochlorophosphine with **3**. Cyclic **2** inserted into the lone P–Cl bond, as shown in eq 7, to form



[(Me₃Si)₂N]₂SnP(Cl)^{*t*}Bu₂ (**12**), which was isolated as yellow crystals in a yield of 88%.

Figure 8 shows the solid-state structure of **12**. Selected bond parameters are given in the figure caption, while data collection

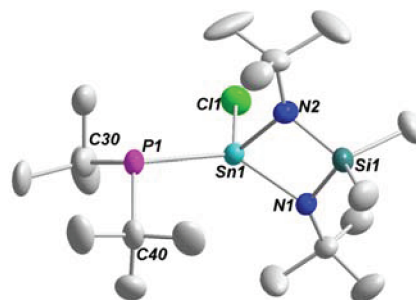


Figure 8. Solid-state structure and partial labeling scheme for **12**, with the major conformation of the P(^{*t*}Bu)₂ moiety shown. Hydrogen atoms have been omitted, and all other atoms are drawn as 50% probability thermal ellipsoids. Selected bond lengths (Å) and angles (deg): Sn1–P1 = 2.4718(10), Sn1–Cl1 = 2.3877(5), Sn1–N1 = 2.0312(17), Sn1–N2 = 2.0371(16); P1–Sn1–Cl1 = 109.84(3), N1–Sn1–N2 = 76.32(7), C30–P1–Sn1 = 108.94(9), C40–P1–Sn1 = 102.8(3), C30–P1–C40 = 110.6(4), N1–Sn1–Cl1 = 107.74(5), N2–Sn1–Cl1 = 107.45(5).

and refinement parameters are given in Table 1. There are two distinct conformations for the Sn–P^{*t*}Bu₂ fragments in the unit cell, both differing substantially in their Sn–P bond lengths. The Sn–P bond in the major conformer is comparatively short (2.4718(10) Å), while that in the minor conformer (2.5945(11) Å) is the longest of any of the compounds described herein. The germylene derivative **13** is depicted in Figure 9 in a perspective that emphasizes the relative sizes of the di-*tert*-butylphosphinyl and chlorogermyl moieties and their orientations with respect to each other. Homologues **12** and **13** join the diinsertion products **9** and **10** as only the second pair of homologous insertion compounds, and here too it was the cyclic heterocarbeneids that gave isolable products. Although the Ge–P and Ge–Cl bonds are slightly elongated, they are not significantly longer than those in **5**, **8**, or **10**.

3.1.3. Reactions of Bis(dichlorophosphino)methane with Group 14 Heterocarbeneids. All the reactions described above involved monophosphines with either one or two chlorine atoms. There are, to our knowledge, no reports on reactions of bis(chlorophosphines) or bis(dichlorophosphines) with group 14 heterocarbeneids. In light of the isolation of the P–P-bonded dimer **6**, the generation of oligomers having [–P–C–P–]_{*n*} segments appeared a conceivable outcome for such interactions. Bis(dichlorophosphino)methane—the simplest bis(dichlorophosphine)—has four P–Cl bonds available for

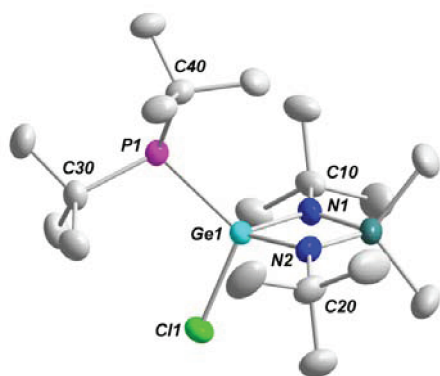
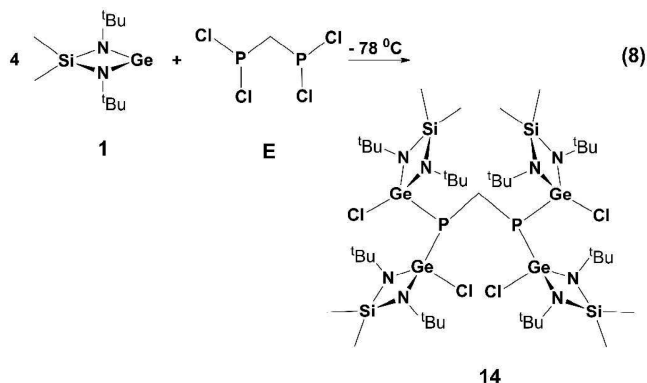


Figure 9. Solid-state structure and partial labeling scheme for **13**. Hydrogen atoms have been omitted, and all other atoms are drawn as 50% probability thermal ellipsoids. Selected bond lengths (Å) and angles (deg): Ge1–P1 = 2.3425(4), Ge1–Cl1 = 2.2170(4), Ge1–N1 = 1.8366(12), Ge1–N2 = 1.8461(12); P1–Ge1–Cl1 = 109.121(17), N1–Ge1–N2 = 83.20(6), C30–P1–Ge1 = 108.41(5), C40–P1–Sn1 = 104.79(5), C30–P1–C40 = 111.65(7), N1–Ge1–Cl1 = 109.09(4), N2–Ge1–Cl1 = 107.46(4).

reaction with heterocarbenes, and a number of scenarios, beginning with monoinsertion and ending with tetrainsertions, seemed plausible.

When we added 2 equiv of **1** to $\text{Cl}_2\text{PCH}_2\text{PCL}_2$, ^{31}P NMR spectroscopy revealed the formation of an unsymmetrical di-insertion product—possibly $[\text{Me}_2\text{Si}(\mu\text{-N}^t\text{Bu})_2\text{Ge}(\text{Cl})]_2\text{-PCH}_2\text{PCL}_2$ —that eluded isolation. When 4 equiv of **1** or **2** was added to hexanes solutions of $\text{Cl}_2\text{PCH}_2\text{PCL}_2$ at -78°C , as shown in eq 8, rapid color changes were observed. ^1H and ^{31}P



NMR spectra on aliquot samples of both mixtures suggested very clean transformations and the presence of only one symmetrical product in each case. Solely in the case of **1**, however, we were able to isolate a stable product: namely **14**. A $^{31}\text{P}\{^1\text{H}\}$ NMR spectrum on the isolated colorless crystals of **14** showed one singlet, shifted to high field (-51.9 ppm) and thereby signaling a product with direct Ge–P bonds.

This was confirmed by a single-crystal X-ray analysis of **14**, the results of which may be seen in Figure 10. The data collection and refinement parameters are given in Table 1, while the figure caption contains selected bond lengths and angles. The molecule crystallized on a 2-fold rotation axis of the tetragonal space group $P\bar{4}$, with the methylene carbon located on that axis. The central methylene group is connected to two bis-(chlorogermyl)phosphines, which enclose a perfectly tetrahedral angle of $108.99(14)^\circ$ at the carbon atom. Despite the substantial steric bulk of the bis(chlorogermyl)phosphino

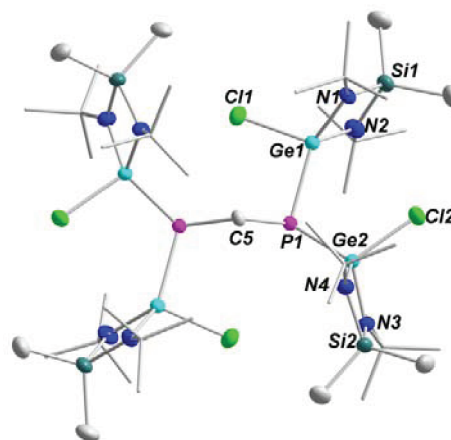


Figure 10. Solid-state structure and partial labeling scheme of C2-symmetric **14**. Hydrogen atoms have been omitted. All other atoms are drawn as 50% probability thermal ellipsoids, except the *tert*-butyl groups, which are shown as sticks for better visibility. Selected bond lengths (Å) and angles (deg): P1–Ge1 = 2.3306(5), P1–Ge2 = 2.3357(5), Ge1–Cl1 = 2.2075(5), Ge2–Cl2 = 2.1979(5), Ge1–N(av) = 1.8249(16), Ge2–N(av) = 1.8338(16), P1–C5 = 1.8699(17); P1–C5–P1' = 108.99(14), Ge1–P1–Ge2 = 108.422(19), P1–Ge1–Cl1 = 95.654(19), P1–Ge2–Cl2 = 105.166(19), N1–Ge1–N2 = 83.56(8), N3–Ge2–N4 = 83.57(8).

groups the phosphorus–carbon bonds have normal lengths (1.8699(17) Å). The two unique phosphorus–germanium bonds are virtually isometric, being 2.3306(5) and 2.3357(5) Å long and almost identical in length with those in **5**. There is a minor discrepancy in the Ge–Cl bonds, the sterically more encumbered Ge1–Cl1 being slightly longer (2.2075(5) Å) than the Ge2–Cl2 bond (2.1979(5) Å), but both bond lengths are comparable to those in **5** and **10**.

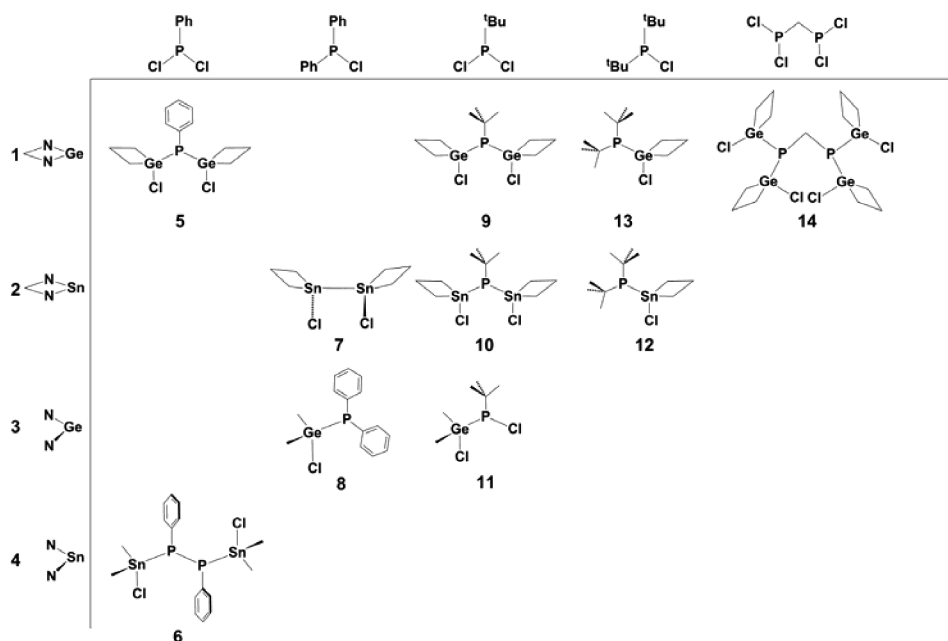
3.2. Product Distribution and Constitution. The thermodynamic products of germylene and stannylene reductions of chloro(organo)phosphines are phosphorus–phosphorus-bonded species (mainly diphosphines and cyclic oligophosphines) and the corresponding dihalides, namely $[(\text{Me}_3\text{Si})_2\text{N}]_2\text{ElCl}_2$ and $\text{Me}_2\text{Si}(\mu\text{-N}^t\text{Bu})_2\text{ElCl}_2$ (El = Ge, Sn). As we showed in the previous section, these reductions proceed with the intermediacy of oxidative addition products of the type $\text{R}_{3-x}\text{P}\{[(\text{Me}_3\text{Si})_2\text{N}]_2\text{ElCl}\}_x$ and $\text{R}_{3-x}\text{P}\{[\text{Me}_2\text{Si}(\mu\text{-N}^t\text{Bu})_2\text{El}]\text{Cl}\}_x$ ($x = 1, 2$; El = Ge, Sn) of varying stabilities.

Because dichlorophosphines can undergo both mono- and di-insertions, the combination of 4 heterocarbenoids and 5 different chloro(organo)phosphines offered the opportunity to potentially isolate more than 20 such insertion products. For a variety of reasons, the major one being kinetic instability, we were unable to obtain all conceivable products for the reactions studied. Nonetheless, 10 intermediates, which are depicted in Table 2, were isolated and fully characterized.

Depending on one's vantage point, the products may be described as either phosphinyl- and chloro-substituted germanium(IV) and tin(IV) compounds or as chlorogermyl- and chlorostannyl-substituted phosphines.³⁴ Because of the ubiquity of phosphines in chemistry, the latter nomenclature is perhaps more appropriate for the compounds shown in Table 2. In the solid state most of the insertion products show remarkable stability to air and elevated temperatures, and even in solution many do not decompose upon prolonged heating.

Phosphorus–germanium bonds are stronger than the corresponding phosphorus–tin bonds, however, and this likely

Table 2. Complete Listing of All Products Isolated from the Reactions of Chloro(organo)phosphines with Cyclic and Acyclic Group 14 Heterocarbenoids^a



^aAll numbered compounds were fully characterized; unnumbered compounds were not structurally characterized by X-ray studies. Empty spaces denote unsuccessful or unattempted reactions.

accounts for the greater stability of the germylene derivatives.^{35,36} As Table 2 shows, there is a preponderance of such species—specifically insertion products involving the cyclic germylene **1**—that is in stark contrast to the two compounds featuring the cyclic stannylene **2**. Compounds **6** and **7** stand out in that they are not true insertion products but rather derived from these intermediates in subsequent reactions. It is significant that both were produced in stannylene, rather than germylene, reductions.

The compounds shown in Table 2 are structural relatives of the insertion products obtained from the interactions of silylenes,^{37,38} germylenes,³⁹ and stannylenes^{40,41} with haloalkanes. Oxidative additions of haloalkanes with group 14 carbenoids, of course, yield products with the much stronger El–C bonds that are less likely to undergo decomposition. Reduction products featuring C–C bonds are therefore rarely isolated.⁴²

An even closer structural relationship exists between the group 14 heterocarbenoids presented herein and N-heterocyclic carbenes (NHCs), although this structural similarity does not translate to reactivity trends. NHCs do not insert into the phosphorus–chlorine bonds, but depending on their steric bulk they either form simple Lewis acid–base adducts with PCl₃ or displace all chlorine substituents as chlorides to furnish cationic phosphorus species with chloride counterions.^{43–46}

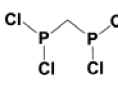
3.3. Reactivity Trends. Perhaps more surprising than the varying stabilities of the insertion products is the very wide range of reaction rates for the oxidative addition reactions, with some being complete in seconds, while at least one interaction showed no product even after being kept at 60 °C for days. Dichlorophosphines can and do undergo diinsertions, and only in the case of **11** were we able to stop the reaction after the first step. In those reactions where diinsertions were observed, the second insertion was almost always slower than the first one, but not significantly so. The half-lives for the various reactions show that, among the chlorophosphines, dichlorophenylphosphine reacts somewhat more quickly than chlorodiphenylphosphine

and bis(dichlorophosphino)methane, while chloroditert-butylphosphine reacts exceedingly slowly, or not at all. Dichloro-*tert*-butylphosphine is intermediate in its reactivity with group 14 heterocarbenoids, the reactions requiring from hours to days in their oxidative additions on these divalent germanium and tin compounds. For any given chlorophosphine, the cyclic stannylene **2** reacted the fastest, while the cyclic germylene **1** and the acyclic stannylene **4** reacted approximately equally quickly, with acyclic germylene **3** being the least reactive. Of the two homologous pairs of heterocarbenoids, **1**, **2** and **3**, **4**, the tin derivatives always reacted noticeably faster than their germanium analogues.

The semikinetic data in Table 3 suggest that steric bulk on both the phosphines and the heterocarbenoids slows the reactions, and this is consistent with an associative mechanism. Group 14 elements have two readily accessible oxidation states (II and IV), the lower oxidation state becoming more stable as one descends the group.^{47–49} Accordingly, the tendency of the group 14 carbenoids to undergo oxidative additions decreases with increasing atomic number of the central element, silylenes being most reactive and plumblylenes least reactive. If the insertion step were the rate-determining step, the germylenes should react more quickly than the stannylenes. The opposite, however, was consistently observed, suggesting that the rate-determining step precedes the oxidative addition. This step likely involves a Lewis acid–base adduct between phosphine and heterocarbenoid. Although we did not detect such intermediates spectroscopically, adducts between electron-deficient group 14 heterocarbenoids and tertiary phosphines are well-known.^{50,51}

The proposed mechanism is analogous to that suggested by du Mont et al. for the insertion of germanium(II) halides into chloro(organo)phosphines,^{11,12} but it differs from those proposed for the reactions of electron-deficient group 14 species with haloalkanes. These latter reactions are generally believed to go by radical pathways.^{38,52,53} We saw no evidence

Table 3. Semi-Kinetic Data (Half-Lives) for the Reactions Investigated in This Study^a

					
	30 min, 0 °C	not attempted	1 d, rt	160 d, 70 °C	20 min, -78 °C
	seconds, -78 °C	seconds, -78 °C	30 min, 0 °C	2 d, 60 °C	seconds, -78 °C
	days, dec.	30 min, 0 °C	1d, rt	not attempted	30 min, -78 °C
	30 min, 0 °C	seconds, 0 °C	1d, rt, dec.	26 d, 70 °C	not attempted

^aReaction rates ranged from immeasurably fast to imperceptibly slow.

in this study that would lead us to propose a radical mechanism for the formation of the insertion products described above. Unlike carbon, phosphorus has a sufficiently high-lying electron pair to form a Lewis acid/base adduct with the electron-deficient carbenoids. To shed more light on the mode of formation and decomposition of the heterocarbenoid insertion products, more detailed kinetic and mechanistic studies are necessary. In particular, we intend to probe the relative importance of steric and electronic substituent effects on phosphorus, because the electron-rich chlorophosphines, e.g., ^tBu₂P-Cl, are also significantly bulkier than the electron-poor ones, e.g., Ph₂P-Cl.

4. CONCLUSION

The homogeneous reductions of monochloro- and dichloro-(organo)phosphines with acyclic and cyclic group 14 heterocarbenoids proceed with the intermediacy of mono- and di-insertion products, respectively. The rates of the insertions vary significantly and depend on both the steric bulk of the reaction partners and on the nature of the group 14 element. Stannylenes always insert more quickly than the homologous germylenes, but stannylene insertion products are also more reactive, resulting in the majority of the isolated intermediates being germanium derivatives. The insertions, which are proposed to follow a coordination/insertion mechanism, are currently being investigated, as are the decomposition pathways of the insertion products.

■ ASSOCIATED CONTENT

Supporting Information

CIF files giving crystallographic data for 5–14. This material is available free of charge via the Internet at <http://pubs.acs.org>.

■ AUTHOR INFORMATION

Corresponding Author

*E-mail: lstahl@chem.und.edu. Tel: 1-701-777-2242. Fax: 1-701-777-2331.

Notes

The authors declare no competing financial interest.

■ ACKNOWLEDGMENTS

We thank the National Science Foundation (Grant No. EPS-0814442) for financial support of this work.

■ REFERENCES

- (1) Dillon, K. B.; Mathey, F.; Nixon, J. F. *Phosphorus: The Carbon Copy*; Wiley: Chichester, U.K., 1998.
- (2) (a) Corbridge, D. E. C. *Phosphorus 2000: Chemistry, Biochemistry, and Technology*, 5th ed.; Elsevier: Amsterdam, 2000. (b) Cowley, A. H. *Chem. Rev.* **1965**, *65*, 617–634.
- (3) Yoshifuji, M.; Shima, I.; Inamoto, N.; Hirotsu, K.; Higuchi, T. *J. Am. Chem. Soc.* **1981**, *103*, 4587–4589.
- (4) Cowley, A. H.; Kilduff, J. E.; Newman, T. H.; Pakulski, M. *J. Am. Chem. Soc.* **1982**, *104*, 5820–5821.
- (5) Shah, S.; Protasiewicz, J. D. *Coord. Chem. Rev.* **2000**, *210*, 181–201.
- (6) Shah, S.; Concolino, T.; Rheingold, A. L.; Protasiewicz, J. D. *Inorg. Chem.* **2000**, *39*, 3860–3867.
- (7) Smith, R. C.; Shah, S.; Protasiewicz, J. D. *J. Organomet. Chem.* **2002**, *646*, 255–261.
- (8) Smith, M. B. *Organic Synthesis*, 2nd ed.; McGraw-Hill: New York, 2002.
- (9) Veith, M.; Huch, V.; Majoral, J.-P.; Bertrand, G.; Manuel, G. *Tetrahedron Lett.* **1983**, *24*, 4219–4222.
- (10) Veith, M.; Grosser, M.; Huch, V. *Z. Anorg. Allg. Chem.* **1984**, *513*, 89–102.
- (11) Karnop, M.; du Mont, W.-W.; Jones, P. G.; Jeske, J. *Chem. Ber.* **1997**, *130*, 1611–1618.
- (12) du Mont, W.-W.; Karnop, M.; Mahnke, J.; Martens, R.; Druckenbrodt, C.; Jeske, J. *Chem. Ber.* **1997**, *130*, 1619–1623.
- (13) du Mont, W.-W.; Neudert, B.; Rudolph, G.; Schumann, H. *Angew. Chem., Int. Ed. Engl.* **1976**, *308*.
- (14) Mathey, F. *Angew. Chem., Int. Ed. Engl.* **1987**, *26*, 275–286.
- (15) Lammertsma, K.; Vlaar, M. J. M. *Eur. J. Org. Chem.* **2002**, 1127–1138.
- (16) Partyka, D. V.; Washington, M. P.; Updegraff, J. B. III; Woloszynek, R. A.; Protasiewicz, J. D. *Angew. Chem., Int. Ed.* **2008**, *47*, 7489–7492.
- (17) Veith, M.; Gouyguou, M.; Detemple, A. *Phosphorus, Sulfur, Silicon Relat. Elem.* **1993**, *75*, 183–186.
- (18) Schweizer, S.; Becht, J.-M.; Le Drian, C. *Org. Lett.* **2007**, *9*, 3777–3780.
- (19) Veith, M. *Angew. Chem., Int. Ed. Engl.* **1975**, *14*, 263–263.
- (20) Veith, M. *Z. Naturforsch.* **1978**, *33b*, 1–6.
- (21) Veith, M.; Grosser, M. *Z. Naturforsch.* **1982**, *32b*, 1375–1381.

(22) Gynane, M. J. S.; Harris, D. H.; Lappert, M. F.; Power, P. P.; Rivière, P.; Rivière-Baudet, M. J. *Chem. Soc., Dalton Trans.* **1977**, 2004–2009.

(23) *SAINT-plus*; Siemens Analytical X-ray Systems, Madison, WI, 1995.

(24) SADABS program for absorption corrections using the Bruker CCD Detector System. Based on: Blessing, R. H. *Acta Crystallogr., Sect. A* **1995**, *51*, 33–38.

(25) Sheldrick, G. M. *Acta Crystallogr., Sect. A* **2008**, *64*, 112–122.

(26) Henderson, W.; Epstein, M.; Seichter, F. J. *Am. Chem. Soc.* **1963**, *85*, 2462–2466.

(27) Dyker, A. C.; Burford, N.; Lumsden, M. D.; Decken, A. J. *Am. Chem. Soc.* **2006**, *128*, 9632–9633.

(28) Geier, J.; Harmer, J.; Grützmacher, H. *Angew. Chem., Int. Ed.* **2004**, *43*, 4093–4097.

(29) Stein, D.; Dransfeld, A.; Flock, M.; Rügger, H.; Grützmacher, H. *Eur. J. Inorg. Chem.* **2006**, 4157–4167.

(30) One of the reviewers correctly pointed out that the distannane **7** could also have been generated from the reaction of a dichloro derivative of **2** with **2** itself.

(31) Pauling, L. *The Nature of the Chemical Bond*, 3rd ed.; Cornell University Press: Ithaca, NY, 1960.

(32) Veith, M. Z. *Naturforsch.* **1978**, *33b*, 7–13.

(33) Baudler, M.; Hahn, J.; Dietsch, H.; Fürstenberg, G. Z. *Naturforsch.* **1976**, *31b*, 1305–1310.

(34) du Mont, W.-W.; Neudert, B. Z. *Anorg. Allg. Chem.* **1977**, *436*, 270–276.

(35) On the basis of the dissociation energies for the P–P (215 kJ/mol),³¹ Ge–Ge (248 kJ/mol), and Sn–Sn (163 kJ/mol) bonds,³⁶ the Ge–P and Sn–P bond dissociation energies are estimated to be 232 and 189 kJ/mol, respectively.

(36) Lappert, M. F.; Pedley, J. B.; Simpson, J.; Spalding, T. R. *J. Organomet. Chem.* **1971**, *29*, 195–208.

(37) Moser, D. F.; Bosse, T.; Olson, J.; Moser, J. L.; Guzei, I. A.; West, R. J. *Am. Chem. Soc.* **2002**, *124*, 4186–4187.

(38) Moser, D. F.; Naka, A.; Guzei, I. A.; Müller, T.; West, R. J. *Am. Chem. Soc.* **2005**, *127*, 14730–14738.

(39) Miller, K. A.; Bartolin, J. M.; O'Neill, R. M.; Sweeder, R. D.; Owens, T. M.; Kampf, J. W.; Banaszak Holl, M. M.; Wells, N. J. *J. Am. Chem. Soc.* **2003**, *125*, 8986–8987.

(40) Lappert, M. F.; Misra, M. C.; Onyszczuk, M.; Rowe, R. S.; Power, P. P.; Slade, M. J. *J. Organomet. Chem.* **1987**, *330*, 31–46.

(41) Veith, M.; Müller, A. J. *J. Organomet. Chem.* **1988**, *342*, 295–301.

(42) Wurtz-type coupling reactions are notable exceptions.

(43) Wang, Y.; Xie, Y.; Abraham, M. Y.; Gilliard, R. J. Jr.; Wei, P.; Schaefer, H. F. III; Schleyer, P. v. R.; Robinson, G. H. *Organometallics* **2010**, *29*, 4778–4780.

(44) Ellis, B. D.; Ragogna, R. J.; Macdonald, C. L. B. *Inorg. Chem.* **2004**, *43*, 7857–7867.

(45) Azouri, M.; Andrieu, J.; Picquet, M.; Cattery, H. *Inorg. Chem.* **2009**, *48*, 1236–1242.

(46) Weigand, J.; Feldmann, K.-O.; Henne, F. D. *J. Am. Chem. Soc.* **2012**, *134*, 0000.

(47) Neumann, W. P. *Chem. Rev.* **1991**, *91*, 311–334.

(48) Mizuhata, Y.; Sasamori, T.; Tokitoh, N. *Chem. Rev.* **2009**, *109*, 3479–3511.

(49) Haaf, M.; Schmedake, T. A.; West, R. *Acc. Chem. Res.* **2000**, *33*, 704–714.

(50) King, R. B. *Inorg. Chem.* **1963**, *2*, 199–200.

(51) Levason, W.; Reid, G.; Zhang, W. *Coord. Chem. Rev.* **2011**, *255*, 1319–1341.

(52) Gynane, M. J. S.; Lappert, M. F.; Miles, S. J.; Power, P. P. *J. Chem. Soc., Chem. Commun.* **1976**, 256–257.

(53) Egorov, M. P.; Gal'inas, A. M.; Basova, A. A.; Nefedov, O. M. *Dokl. Akad. Nauk* **1993**, *329*, 594–595.